Computational Biology Exposed a Common Pathogenic Mechanism in Influenza A and Guillain-Barré Syndrome

Ye Deng [1,¶], Zhongwen Tang [1,3,¶], Qiong Chen [4,¶], Xujuan Hu [1], Ying Jie Zhang [1], Meng Chen[5], Qiongya Wang [1,*], Fuli Ren [1,2,*]

[1] Clinical Biological Biospecimen Resource Center, Wuhan Jinyintan Hospital, Tongji Medical College of Huazhong University of Science and Technology, Wuhan, Hubei, China

[2] State Key Laboratory for Diagnosis and Treatment of Severe Zoonotic Infectious Diseases, Wuhan, Hubei, China.

[3] Department of Thoracic Surgery,Wuhan Jinyintan Hospital, Tongji Medical College of Huazhong University of Science and Technology, Wuhan, Hubei, China

[4] Department of Gastroenterology, Wuhan Children's Hospital, Tongji Medical College of Huazhong University of Science and Technology,Wuhan, Hubei, China

[5] Institute of Aging, Wenzhou Medical University, Wenzhou, China

[*] Corresponding author

Email:renny08@163.com

[¶] These authors contributed equally to this work.

Abstract

Influenza A (H1N1) is an acute respiratory infection, while Guillain-Barré syndrome (GBS) is an autoimmune peripheral neuropathy that can occur as a post-infectious complication. Clinical evidence suggests a potential link between H1N1 infection and subsequent GBS development, implying common immunopathological mechanisms. To explore this, we integrated bioinformatics and systems biology approaches to analyze transcriptome data from H1N1 and GBS patients in the GEO database, and 32 common differentially expressed genes (DEGs) were identified . Subsequent Gene Ontology (GO) and Kyoto Encyclopedia of Genes and Genomes (KEGG) pathway enrichment analyses revealed key functional associations for these DEGs. Protein-protein interaction (PPI) network analysis highlighted TLR4, TNF, and ITGAM as central hub genes, uncovering potential shared molecular pathways between H1N1 and GBS. Furthermore, analysis of hub gene interactions with microRNAs (miRNAs), transcription factors (TFs), and related diseases facilitated the prediction of potential therapeutic drugs. Molecular docking simulations were performed to validate predicted drug interactions with the hub gene products. Collectively, these findings delineate shared molecular mechanisms and provide insights for targeted therapy in patients developing GBS post-H1N1 infection.

Introduction

Influenza A is an acute respiratory infection caused by influenza A viruses, and its global epidemic infects millions of people each year, with significant morbidity and mortality.[1, 2] H1N1, the most prevalent subtype of the influenza A virus, has been demonstrated to induce the release of cytokines and trigger an inflammatory response through the activation of both innate and adaptive immune responses in the host, resulting in respiratory symptoms and systemic complications[3]. Guillain-Barré syndrome (GBS) is a post-infectious autoimmune peripheral neuropathy characterised by acute flaccid paralysis. This condition is associated with molecular mimicry or a cross-immune response, which causes the immune system to attack the myelin sheath or axons of peripheral nerves[4]. A substantial body of research in the field of epidemiology has demonstrated that between 20 and 30 percent of patients diagnosed with Guillain-Barré syndrome (GBS) have experienced a secondary onset of the condition following a viral or bacterial infection. Among the various causative agents identified,

influenza virus has been identified as a significant trigger for this secondary manifestation. For instance, during the 2009 influenza A H1N1 pandemic, the incidence of Guillain-Barré syndrome (GBS) increased significantly, further suggesting a potential association between the two in immunopathological mechanisms[5].

Whilst clinical observations support a temporal association between influenza and GBS, the molecular mechanism between the two remains unclear. A paucity of research has hitherto been conducted on the common pathogenic network across diseases, with the majority of studies focusing on the immune or genetic characteristics of a single disease. For instance, research has been conducted on the activation of interferon signalling pathways in influenza A or the role of anti-ganglioside antibodies in GBS. Furthermore, extant treatment strategies principally target immune abnormalities in GBS, but prophylactic or targeted interventions for post-influenza A GBS remain limited[6]. In recent years, bioinformatics and systems biology approaches have demonstrated unique advantages in the identification of molecular interaction networks in complex diseases. These approaches include the identification of core regulatory modules through the integration of multi-omics data and the utilisation of machine learning models to predict potential therapeutic targets. However, the application of such methods in the crossover study of H1N1 and GBS has not been fully explored.

The objective of this study was to investigate the co-pathogenesis of influenza A H1N1 virus infection and GBS, and to explore potential therapeutic agents. Firstly, the GEO database transcriptome datasets of H1N1 and GBS were analysed to identify the DEGs of the two diseases, respectively, and then the common DEGs were obtained by comparison. It is vital to note that, we did not use these common differentially expressed genes (DEGs) for gene ontology (GO) functional annotation and Kyoto Encyclopedia of Genes and Genomes (KEGG) pathway enrichment analysis, as the platforms of the two datasets used were different and there was a gap in data volume. In this study, GO and KEGG of the two datasets were analyzed separately. Then take the intersection according to the degree of importance. Subsequently, the PPI network was constructed, hub genes were screened out by topological analysis, and the key genes with the highest connectivity were selected for further study. In order to verify the clinical value of this key gene, the regulatory mechanism of common DEGs in H1N1 infection was revealed through transcription factor-target gene interaction network analysis. Finally, the database analysis yielded the drugs associated with the hub genes, and then used the obtained drug molecules to perform simulated docking experiments with the target protein molecules of H1N1 and GBS. The experimental workflow, from data collection to analysis, is depicted in Fig 1

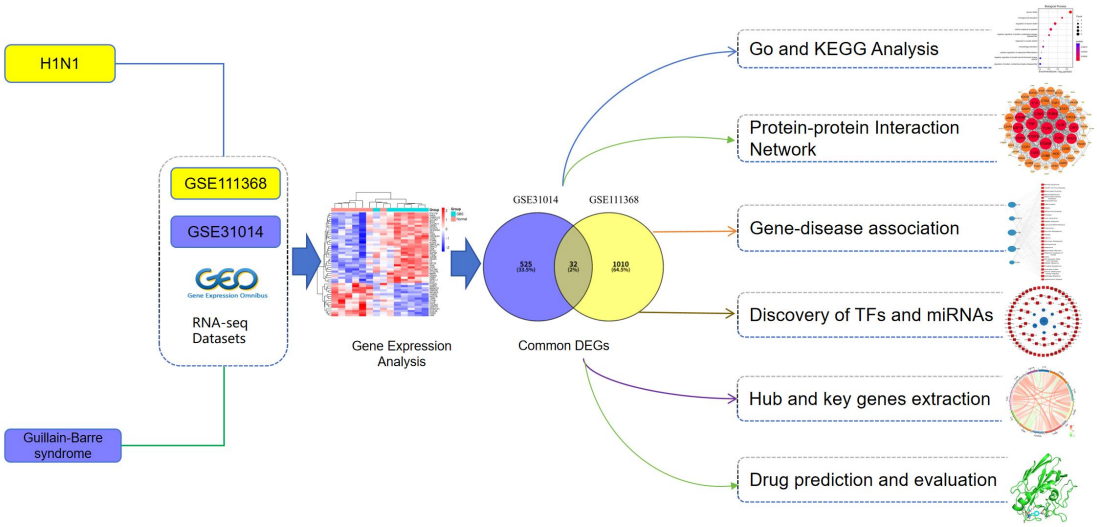

Fig 1. Schematic diagram of the research process in this paper.

Materials and Methods

The GEO database (https://www.ncbi.nlm.nih.gov/geo/) was accessed, and the GSE111368 dataset was selected, which was generated on the GPL10558 microarray platform (Illumina HumanHT-12 V4.0)[7]. The dataset under consideration contains 109 samples infected with influenza A (H1N1) and 130 samples from healthy subjects. The sequencing platform utilised the Illumina Human HT-12 V4.0 expression microarray chip. The GSE31014 dataset was generated using the GPL96 platform (Affymetrix Human Genome U133A Array [HG-U133A]), comprising seven GBS patient samples and seven healthy control samples [8-9]. The identification of disease-associated DEGs was achieved through a comparative analysis of the GSE111368 (H1N1 infection) and GSE31014 (GBS) mRNA datasets. Utilising the limma R package in conjunction with empirical Bayes moderation, we implemented linear models to extract differentially expressed genes (DEGs) for each disease. The selection of statistically significant genes was undertaken utilising dual thresholds. Benjamini-Hochberg adjusted $P < 0.05$ was employed for false discovery rate control and absolute log2 fold-change (log2FC) ≥ 1. Finally, shared DEGs between the two datasets were identified via the VENN v2.1 online tool (https://bioinfogp.cnb.csic.es/tools/venny/) [10-11].

Functional enrichment analysis of common DEGs

82 Functional enrichment analysis is a bioinformatics approach that identifies statistically overrepresented biological
83 annotations with the aim of elucidating the potential mechanisms of DEGs. The method under scrutiny has been
84 demonstrated to detect significant enrichment of GO terms, KEGG pathways and disease-associated signatures. This
85 capability enables the delineation of the functional contributions of specific gene collections to particular pathophysiological
86 processes. In this study, we conducted go and pathways analyses on H1N1 infection and GBS respectively. Among the
87 documents obtained from the go analyses and pathways analyses of both, the top ten significant common functions and
88 pathways were selected based on the minimum adjusted P-value as the ranking criterion to explore the common molecular
89 mechanisms of these two diseases.

90 Specifically, we used GO analysis to functionally classify common DEGs, including biological processes (BP),
91 molecular function (MF), and cellular components (CC), to clarify their roles in key pathological processes such as immune
92 regulation and neuroinflammation. At the same time, based on KEGG pathway enrichment analysis, the signaling pathways
93 involved in these genes (such as virus-host interaction, autoimmune response, etc.) were further analyzed, so as to further
94 discover the potential association mechanism between H1N1 infection and the pathogenesis of GBS[11-13].

95 **Protein-protein interaction network analysis**

96 Proteins execute their mechanistic roles within cellular systems through interactions in protein-protein interaction
97 (PPI) networks. To elucidate disease-related protein functions, we constructed PPI networks using common DEGs for
98 subsequent interaction analysis[14]. The analysis was performed using STRING (v12.0; https://www.string-db.org/), a
99 comprehensive database of known and predicted protein associations, including physical interactions and functional linkages.
100 Common DEGs were entered into STRING and a confidence threshold (composite score > 0.4) was applied to generate PPI
101 networks[15, 16].

102 The PPI networks were imported into Cytoscape (v3.10.3) for visualization and downstream analysis. Hub genes
103 were identified using CytoHubba, a Cytoscape plugin that calculates 12 network centrality algorithms to rank node
104 importance[14,17]. Based on validation studies demonstrating its superior discriminative power, the Maximum Clique
105 Centrality (MCC) method was selected to extract the twelve most significant hub genes..

106 **Transcriptional Regulatory Network Mapping via TF and miRNA Interactions**

107 To decode the transcriptional regulatory architecture underlying shared DEGs in H1N1 influenza and GBS, we
108 leveraged the NetworkAnalyst platform (https://www.networkanalyst.ca/) for multi-omics integration[18]. Firstly, we utilized

109 the JASPAR database to identify reliable transcription factor binding sites, and at the same time combined the experimentally
110 validated miRNA-target gene interactions data in miRTarBase and TarBase[19-21]. We constructed a comprehensive DEG-
111 TF-miRNA regulatory network; subsequently, we used Cytoscape (v3.10.3) to perform network visualization and analysis,
112 focusing on the screening of core transcription factors and key miRNAs that regulate multiple common DEGs, and these
113 regulatory nodes may be involved in the common pathogenesis of the two diseases by influencing processes such as virus-
114 host interactions and neuroimmune regulation.

115 **Gene-disease association analysis networks**

116 The DisGeNET database (https://www.disgenet.org/) was utilised to construct gene-disease association networks,
117 with molecular relationships being systematically aggregated from experimental data, GWAS repositories, and curated
118 literature evidence [22]. The NetworkAnalyst platform was utilised to integrate these associations with multi-omics networks.
119 This facilitated the delineation of disease mechanisms and enabled the construction of comorbidity networks between H1N1
120 and GBS.

121 **Therapeutic Compound Screening via Gene Signature Drug Repositioning**

122 We predicted protein-drug interactions (PDIs) and identified repurposable therapeutic agents by targeting common
123 DEGs shared between H1N1 influenza and GBS. Using the Drug Signature Database (DSigDB) embedded within the Enrichr
124 platform, we performed gene set enrichment analysis to discover compounds significantly associated with these DEG
125 signatures (FDR<0.05)[23]. The Enrichr repository (http://amp.pharm.mssm.edu/Enrichr) provides comprehensive, genome-
126 scale gene set libraries for enrichment analysis, with DSigDB specifically curating drug/compound-target gene relationships
127 accessible through its Disease/Drug Functions module[24].

128 **Structure-Based Virtual Screening via Molecular Docking**

129 Molecular docking, a computational drug discovery approach predicting ligand-target binding modes, was employed
130 to identify therapeutic compounds and establish structure-activity relationships without prior knowledge of target modulators
131 [25]. Specifically for this study, we selected H1N1 viral targets—including receptor-binding proteins (hemagglutinin/HA,
132 neuraminidase/NA) and functional non-receptor proteins (M2 ion channel regulating endosomal pH, nucleoprotein/NP for
133 RNA packaging)—alongside GBS-associated targets (gangliosides, myelin proteins) through systematic literature analysis.
134 High-resolution crystal structures were retrieved from the PDB database (via NCBI) and compound libraries from PubChem.

135 Using the CB-Dock2 platform implementing cavity-detection guided blind docking (https://cadd.labshare.cn/cb-dock2), we
136 performed energy minimization of protein structures with the AMBER force field prior to docking simulations. Binding
137 affinity was quantitatively evaluated by weighted-average Binding Energy (BE) scoring, where BE ≤ -8.0 kcal/mol indicated
138 high-affinity interactions. Finally, binding poses were analyzed in PyMOL v2.5.5 with critical intermolecular distances (H-
139 bond/π-π stacking < 3.5Å) measured, though molecular dynamics simulations were not conducted for conformational
140 validation.

141 Result

142 **Identification of common gene expression signatures between H1N1 and GBS**

143 Severe H1N1 influenza infection has been observed to trigger GBS in susceptible individuals during the post-
144 infection immune dysregulation phase (5 days to 3 weeks) through molecular mimicry mechanisms analogous to
145 Campylobacter jejuni pathogenesis. However, further characterisation is required to determine the specific influenza-specific
146 antigenic targets involved in this process. It is noteworthy that patients who developed GBS following H1N1 infection
147 exhibited doubled mortality rates compared to classical GBS cases. This phenomenon can be attributed to the exacerbation of
148 respiratory compromise and autonomic dysfunction.

149 Transcriptomic profiling of peripheral blood samples (GSE111368, H1N1; GSE31014, GBS) identified 1,042
150 differentially expressed genes (DEGs), with 141 being found to be upregulated and 175 downregulated in H1N1, and 40
151 being found to be upregulated and 517 downregulated in GBS. Volcano plots illustrated prominent expression shifts in both
152 conditions (Fig. 2A-B), while hierarchical clustering heatmaps revealed distinct disease-specific signatures (Fig. 2C-D). Of
153 particular significance was the observation that the 12 most significantly dysregulated H1N1-associated DEGs converged on
154 neuroinflammatory pathways and immune response regulation, suggesting shared mechanistic underpinnings. Venn analysis
155 (Fig. 2E) delineated 32 conserved DEGs between the two conditions. A comprehensive investigation into the functional
156 annotation of these overlapping signatures has revealed that there are some commonalities in the functional mechanisms and
157 interactions between H1N1 and GBS.

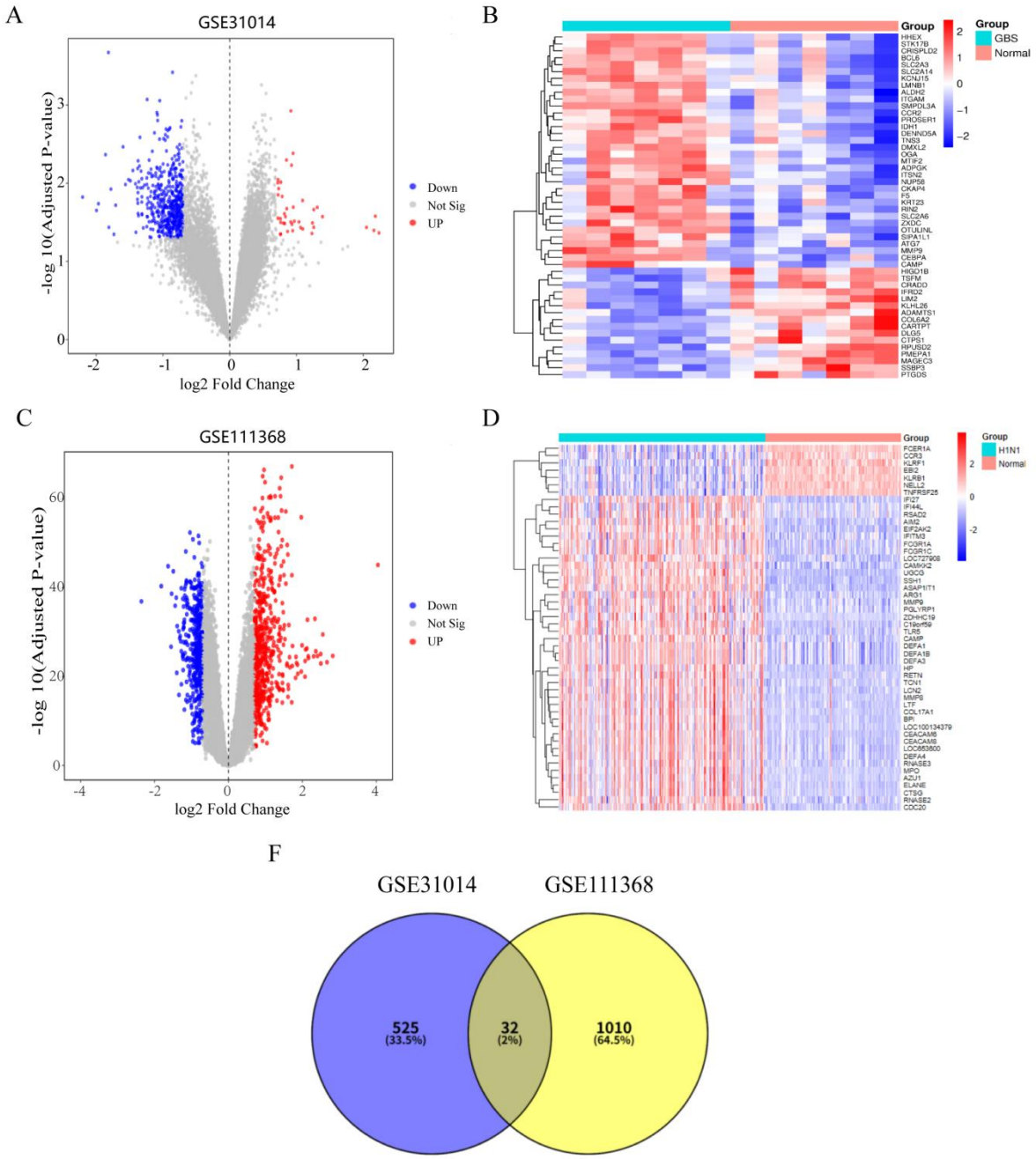

Fig 2. Differential gene expression profiling in Guillain-Barré syndrome (GBS) and H1N1 influenza datasets. (A) Volcano plot of DEGs in GBS dataset (red: up-regulated; blue: down-regulated; gray: non-significant genes; P<0.05). (B) Heatmap clustering analysis of top 50 DEGs in GBS. (C) Volcano plot of DEGs in H1N1 dataset. (D) Heatmap clustering analysis of top 50 DEGs in H1N1. (F) Venn diagram of common DEGs between GSE31014 and GSE111368 datasets.

Functional enrichment analysis of differentially expressed genes

As illustrated in Fig 3A-B, bubble plots are employed to present the results of gene ontology (GO) enrichment analysis, which is categorised into three distinct groups. The following three categories are to be considered: biological process (BP), cellular component (CC), and molecular function (MF). In these visualisations, colour depth corresponds to statistical significance (-log10(p-value)), while the size of each bubble reflects the number of genes in each term. Specifically, the results of the BP in Fig 3A analysis revealed highly enriched immune responses: Items such as Gram-positive bacterial defense response, antibacterial humoral response, and viral defense response are red in color and have a large number of genes, indicating a significant enrichment of immune defense-related genes. The research subjects may be in a state of pathogen stimulation and immune activation. Fig 3B presents a multi-dimensional functional analysis of the genes based on GO enrichment. In the biological process (BP) category, the enrichment of immune defense response pathways confirms their central role in the immune response, indicating that the research subjects may be under pathogenic stimulation or in a state of immune activation. Both graphs point to "significant activation of the immune defense response" and the two figures from different visualization forms jointly verify that the immune defense response is the core functional enrichment direction of the research object.

The Fig 3C-D presents a visual synthesis of KEGG signaling pathway enrichment analysis results and gene-pathway association profiles. In Fig 3C, results demonstrate significant activation of immune response, hypoxic adaptation, and tumor immunity-associated pathways (FDR < 0.05), suggesting that immune activation, a hypoxic microenvironment, or a tumor-associated state aligns with the clinical symptoms of influenza and GBS patients. In Fig 3D, 37 genes, including KRT23, MMP9, CXCL8, TLR8, PIK3CA, MAPK3, etc., were mapped to 10 core signaling pathways through Sankey junction lines. Among them, Toll-like receptor signaling pathways involving LY96, TLR8, TICAM2, chemokine signaling pathways enriched CXCL8 and DOCK2, and T cell receptor signaling pathways CD40LG, LCP2, and NFATC1 showed high correlations. In particular, the simultaneous enrichment of PD-L1/PD-1 cancer immune checkpoint pathways such as PIK3CA and PIK3R1 and AMPK/mTOR metabolic pathways such as PDK1 and RPS6KB1 suggests a possible synergistic effect between metabolic reprogramming and immune escape mechanisms. Collectively, these findings integrate across Fig 3A-D to identify functional convergence in neurodegenerative processes and anti-viral immune responses through coordinated dysregulation of shared gene networks.

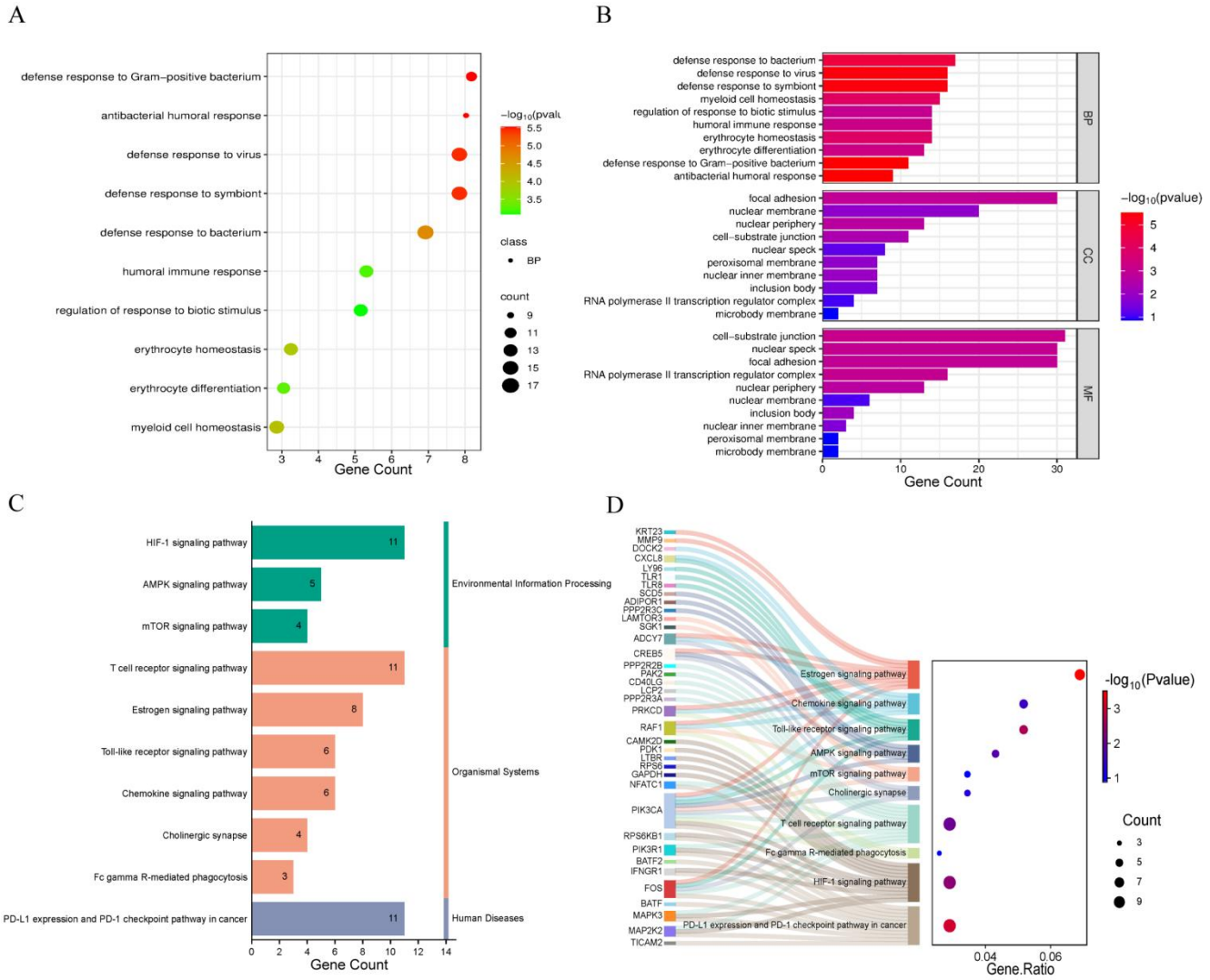

Fig 3. The significance analysis results obtained by analyzing the gene Ontology (GO) and KEGG evaluations of the two datasets. (A) Scatter plot visualization of BP terms significantly enriched by GO analysis. (B) The bar chart of Gene Ontology (GO) enrichment analysis divided into BP (Biological Process), CC (Cellular Component), MF (Molecular Function). (C) Bar chart depicting the results of KEGG pathway enrichment analysis for the overlapping pathways identified in the two datasets.. (D) Sankey diagram visualizing the enrichment relationships of shared KEGG pathways between the two datasets.

Protein Interaction Network Analysis Reveals Core Molecular Drivers

A protein-protein interaction (PPI) network was constructed using the 32 common differentially expressed genes (DEGs) that were identified as being differentially expressed between H1N1 influenza and Guillain-Barré syndrome (GBS). The network under consideration (Fig. 4A) was constructed utilising the STRING database and subsequently visualised in Cytoscape v3.10.3. The network comprises 73 nodes interconnected by 770 edges, with the size and colour intensity of the nodes correlating with their interaction centrality. It can be observed that larger, darker nodes indicate greater functional significance. A comprehensive topological analysis was conducted using five distinct algorithms (MCC, Degree, MCN, Closeness, DMNC) with CytoHubba, which resulted in the identification of pivotal regulatory genes. The Maximal Clique Centrality (MCC) method was employed to identify 32 genes of particular significance in the context of the study. Convergence across all algorithms led to the identification of 10 core overlapping regulators: TLR4, ITGAM, TNF, FCGR3A, CD8A, IL1B, TLR2, TLR8, CSF1R, IL10, and STAT3 (see Table 1 for complete rankings). Submodule analysis in Fig. 4B demonstrates tight functional clustering among these hub genes, with TLR4—a pathogen recognition receptor critical for innate immune activation (NCBI Gene:7099)—emerging as the highest-connectivity node.

Further characterisation included the creation of a Venn diagram (Fig. 4C), which confirmed a high level of concordance between the algorithms in terms of Degree centrality values. Additionally, gene co-expression networks were constructed via gene co-expression network analysis (GCNA) for the top 12 ranked genes (Fig. 4D). The integrated results of this study establish that TLR-mediated immune activation and cytokine signalling pathways are central mechanisms that link viral infection and the pathogenesis of autoimmune neuropathy.

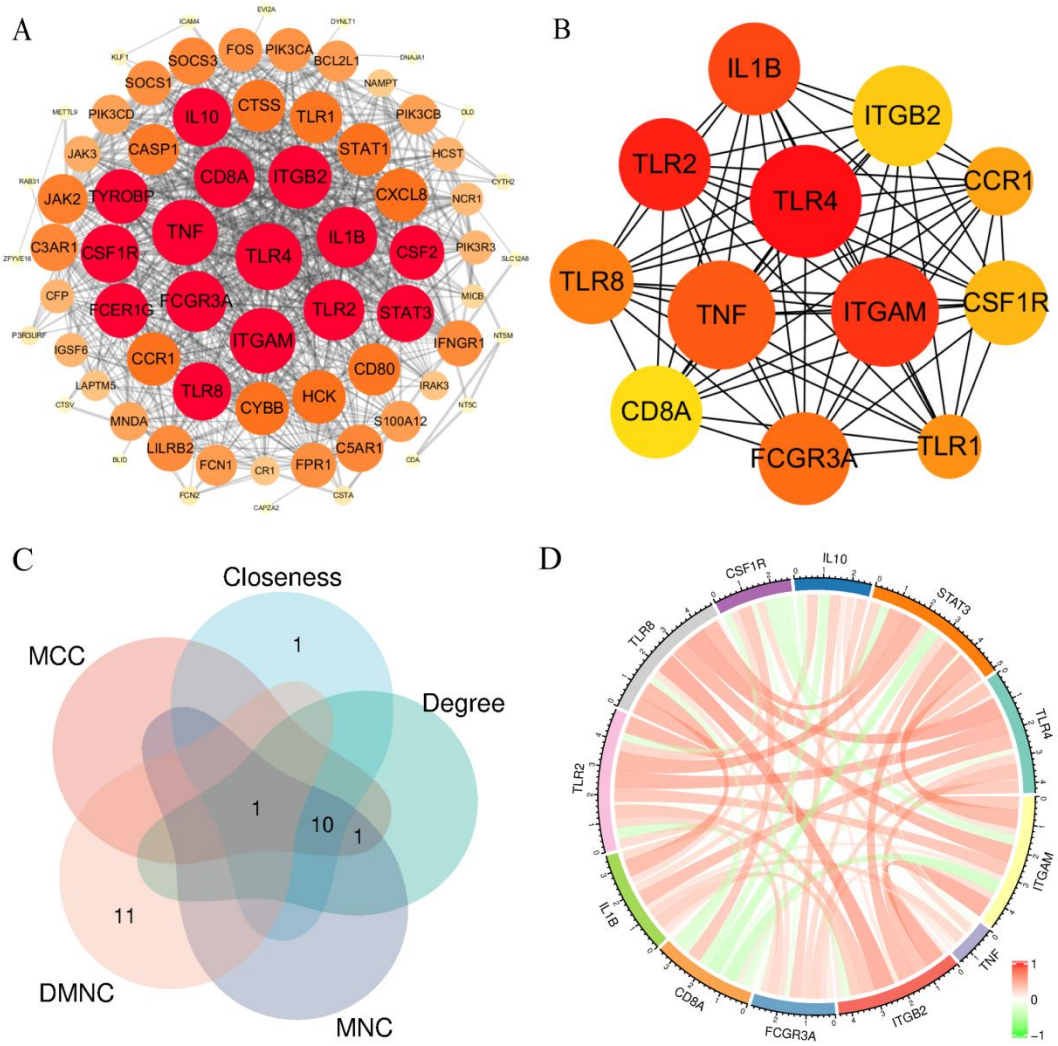

Fig 4. Hub gene identification and interaction analysis. (A) Protein-protein interaction network of 32 shared differentially expressed genes (DEGs) visualized in Cytoscape. (B) Key functional clusters identified through MCC algorithm screening. (C) Intersection of hub genes derived from five distinct computational methods (Venn diagram). (D) Co-expression network of the top 12 hub genes ranked by MCC algorithm scores.

Table 1. CytoHubba's AlphaMc using five algorithms (MCC, Closeness, Degree, MNC, and DMNC)

MCC	Closeness	Degree	MNC	DMNC
TLR4	TLR4	TLR4	TLR4	TLR1
ITGAM	TNF	TNF	ITGAM	FPR1

TNF	ITGAM	ITGAM	TNF	LILRB2
ITGB2	ITGB	ITGB2	ITGB2	MNDA
FCGR3A	IL1B	IL1B	IL1B	CCR1
CD8A	TLR2	TLR2	TLR2	FOS
IL1B	FCGR3A	FCGR3A	FCGR3A	CASP1
TLR2	CD8A	CD8A	CD8A	C5AR1
TLR8	IL10	IL10	IL10	IGSF6
CSF1R	CSF1R	CSF1R	CSF1R	CYBB
IL10	TLR8	TLR8	TLR8	C3AR1
STAT3	STAT3	STAT3	STAT3	TLR2

Differential expression analysis of GBS-H1N1 common DEGs

The expression profiling of key genes across H1N1 influenza and GBS datasets revealed significant upregulation of TLR4 in GBS samples relative to controls (Figs. 5A-B). This finding is consistent with the established role of TLR4 in pathogen recognition via LPS sensing and innate immune activation. A correlation analysis of shared differentially expressed genes was conducted, which identified TLR8 and ITGB2 as exhibiting the strongest positive relationship (r=0.78, Fig. 5C). This finding suggests that TLR8-mediated viral RNA recognition may upregulate ITGB2, thereby enhancing immune cell adhesion and migration during the process of pathogen clearance. The finding is mechanistically reinforced by the co-regulation of TLR4 and TLR8 (r=0.76), indicating synergistic activation during co-infections that amplifies production of pro-inflammatory cytokines, including TNF-α and IL-6. As illustrated in Figure 5D, ITGB2 demonstrates predominant expression in both disease contexts. In the context of H1N1 infection, this phenomenon may be indicative of viral activation of TLR3/7/8 and RIG-I pathways in myeloid cells, thereby promoting the formation of the ITGB2-integrin complex (CD11b/CD11a), which in turn facilitates the trafficking of immune cells. In contrast, elevated ITGB2 levels in GBS are associated with anti-ganglioside antibody-mediated complement activation. This process involves the recruitment of ITGB2-expressing macrophages and T-cells to peripheral nerves, where they induce demyelination and axonal damage. This correlation has been further substantiated in experimental autoimmune neuritis models, which demonstrate that ITGB2 expression levels are directly proportional to the severity of neuroinflammation. The integrated findings establish a

continuum wherein viral-triggered immune mechanisms converge with autoimmune processes through dysregulation of shared molecular pathways involving TLR signalling and integrin-mediated inflammation.

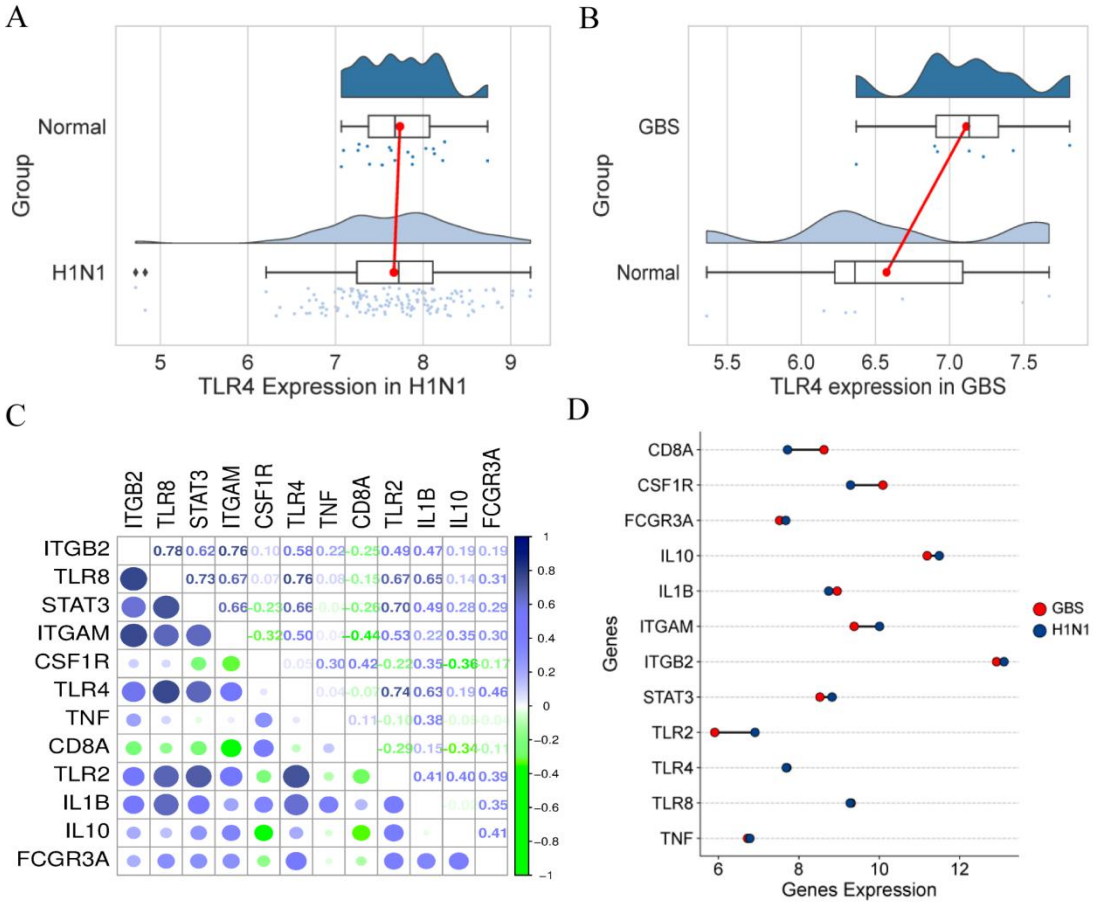

Fig 5. Expression patterns and correlations of key genes in H1N1 and Guillain-Barré syndrome (GBS) datasets. (A-B) Differential expression of TLR4 in H1N1 (A) and GBS (B) datasets. (C) Correlation matrix of significantly DEGs. (D) Comparative expression profiling of key DEGs across H1N1 and GBS datasets.

Transcriptional and Post-transcriptional Regulatory Networks of Core H1N1-GBS Genes

In order to elucidate the transcriptional-level regulation of common differentially expressed genes (DEGs), integrated regulatory networks were constructed, mapping transcription factors (TFs) and microRNAs (miRNAs) through

TarBase and miRTarBase databases. As illustrated in Figures 6A-B, the DEG-TF interaction network is visualised, whereby circular nodes represent DEGs and square nodes denote TFs. The size of each node is scaled by its connectivity degree, with larger nodes indicating critical network hubs. Key DEGs with high connectivity (TLR4, STAT3, TNF, ITGAM, IL-10) demonstrate multifaceted roles; a. TLR4 (a key innate immune receptor) detects pathogens and modulates inflammatory responses during H1N1 infection, while its elevated expression in GBS patients correlates with disease severity; b. STAT3 compensated for H1N1 NS1-mediated STAT1 inhibition, thereby maintaining antiviral defences. Furthermore, the research revealed that STAT3 inhibitors attenuated GBS-like neuroinflammation in animal models [26]. Among the transcription factors (TFs) analysed, NF-κB, JUN, SP1, GATA3, and HSF1 exhibited the highest regulatory significance..

Complementary networks of differentially expressed genes (DEGs) and microRNA (miRNA) (Fig. 6C) identified seven genes (STAT3, IL-1β, IL-10, TLR4, TNF, ITGB2, CSF1R) with the strongest interactions between DEGs and miRNAs. The hub miRNAs included hsa-miR-34a-5p, hsa-miR-98-5p, hsa-miR-19a-3p, hsa-miR-27a-3p, and hsa-miR-25a-3p. It is of crucial importance to note that hsa-miR-34a-5p has been observed to exhibit dual pathological roles. Firstly, in cases of H1N1, it has been demonstrated to attenuate cytokine storms by inhibiting NF-κB. In Guillain-Barré syndrome (GBS), it has been demonstrated that this exacerbates autoimmunity by promoting Th17/M1 polarization, which has been shown to positively correlate with disease severity [27]. This suggests that its inhibition could promote neural repair.

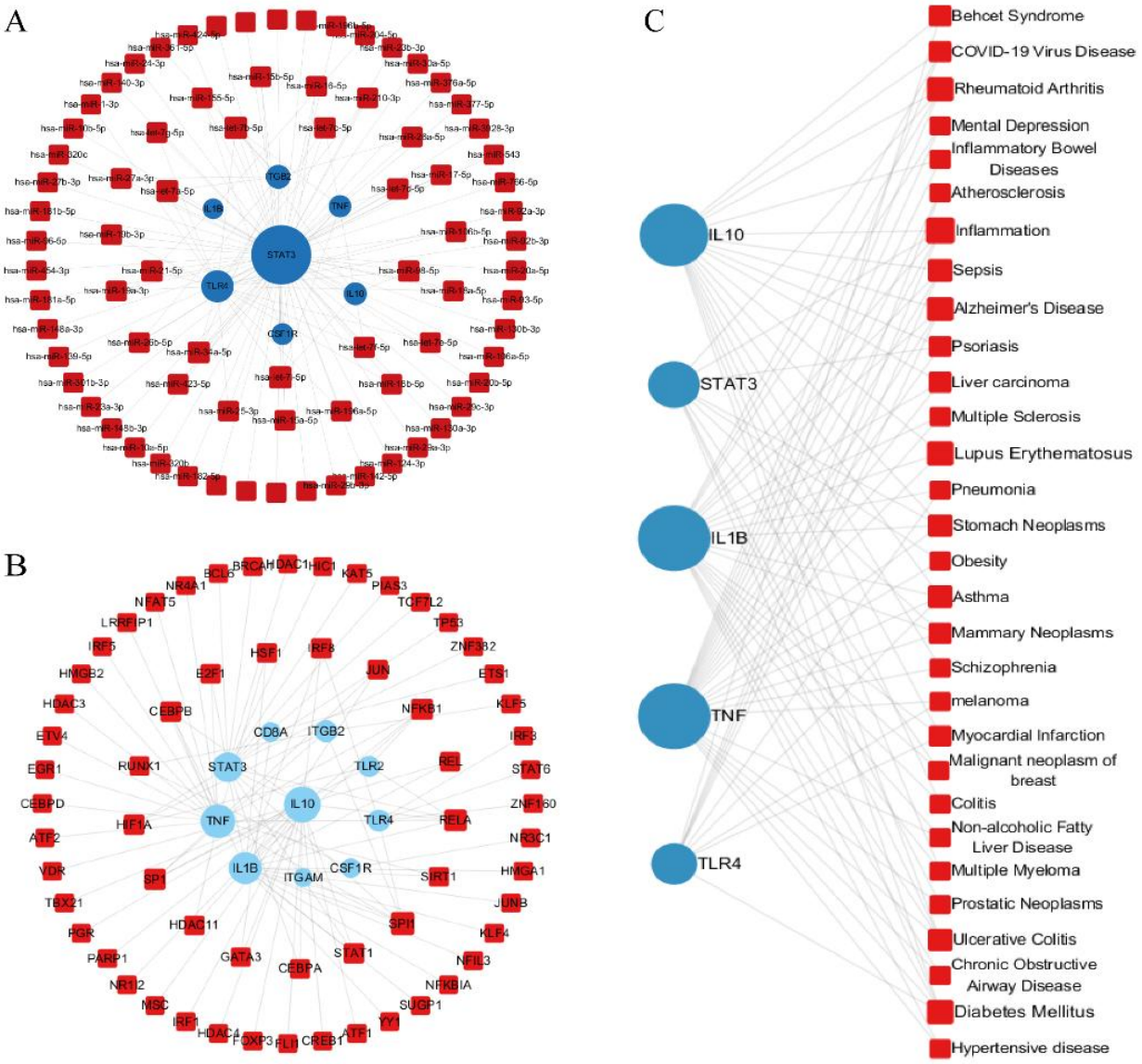

Fig 6. Regulatory networks illustrating interactions among DEGs, miRNAs, transcription factors (TFs), and diseases. (A) DEGs-miRNA regulatory network: Blue circular nodes represent differentially expressed genes (DEGs); red square nodes represent miRNAs. (B) DEGs-TF interaction network: Blue circular nodes indicate DEGs; red square nodes denote transcription factors. (C) Gene-disease association network: Blue circular nodes show DEGs; red square nodes represent disease entities.

Therapeutic Discovery Validated by Multi-Target Molecular Docking

281 Our molecular docking strategy targeted pathophysiologically critical proteins: H1N1 surface glycoproteins
282 hemagglutinin (HA) and neuraminidase (NA) mediating viral-host adhesion [38], alongside GBS autoantigen myelin protein
283 zero (MPZ) – constituting 50-70% of peripheral nerve myelin and triggering demyelination in experimental autoimmune
284 neuritis (EAN) models [39-40]. The details of six potential drug molecules include Parthenolide, Betulinic acid, Tofacitinib,
285 Liuzasulfapyridine, Naringenin and Leucovorin are shown in Table 2. Binding analyses across all prioritized compounds
286 revealed:

287 Parthenolide formed hydrogen bonds with NA catalytic residues (Fig 7A), validating its replication inhibition [30],
288 while hydrophobic interactions stabilized MPZ (Fig 7B), supporting neuroregeneration [33]. Betulinic acid occupied NA's
289 sialic acid pocket (Fig 7C) via van der Waals forces [34], and anchored MPZ transmembrane domains (Fig 7D) to attenuate
290 neuroinflammation [35].

291 Tofacitinib established salt bridges with NA (Fig 7E), corroborating JAK-STAT blockade [36], while hydrogen
292 bonding to MPZ extracellular loops (Fig 7F) aligned with immunomodulation [37]. Naringenin formed π-π stacking with NA
293 active sites (Fig 7G) and stabilized MPZ dimers (Fig 7H), indicating flavonoid-mediated membrane stabilization.

294 Sulfasalazine exhibited π-cation interactions with both NA (Fig 7I) and MPZ (Fig 7J), suggesting novel target
295 engagement. Chelidonine, an isoquinoline alkaloid – demonstrated unanticipated binding to NA catalytic triad (Fig 7K) and
296 MPZ immunoglobulin domains (Fig 7L), warranting further exploration.

297

298 **Table 2. Candidate drugs determined by comprehensive analysis from the CMAP database of gene-Drug interactions**
299 **and the DSigDB database (ranked by possibility in the top 6)**

High probability associated drugs

Drugs	Associated direction	Key basis	Compound molecular formula
Parthenolide	H1N1 (Anti-inflammatory), GBS (neuroprotective)	Inhibit the NLRP3 inflammasome and reduce cytokine storms; Neural anti-inflammatory effects were shown in animal models.	$C_{26}H_{28}N^{3+}$
Betulinic Acid	H1N1 (Antiviral/Anti-inflammatory)	Broad-spectrum antiviral (destroying the envelope), inhibiting NF-κB, and possibly alleviating influenza lung injury.	$C_{30}H_{48}O_3$

Tofacitinib Citrate	GBS (Immune Regulation)	JAK3 inhibitors, similar to tofacitinib, can inhibit autoreactive T cells (potentially for autoimmune neuropathy).	$C_{22}H_{28}N_6O_8$
Moderate possibility associated drugs			
Drugs	**Associated direction**	**Key basis**	**Compound molecular formula**
Naringenin	H1N1 (Auxiliary anti-inflammatory)	Antioxidant, reduces influenza-associated oxidative stress, but weak direct antiviral effect.	$C_{15}H_{12}O_5$
Sulfasalazine	H1N1 (immunomodulation)	Inhibition of NF-κB, which may alleviate excessive inflammation, but no direct antiviral data.	$C_{18}H_{14}N_4O_5S$
(+)-Chelidonine	GBS (theoretical neuroprotection)	Anti-inflammatory and microtubule inhibitory effects, but high toxicity and need for structural modification.	$C_{20}H_{19}NO_5$

300

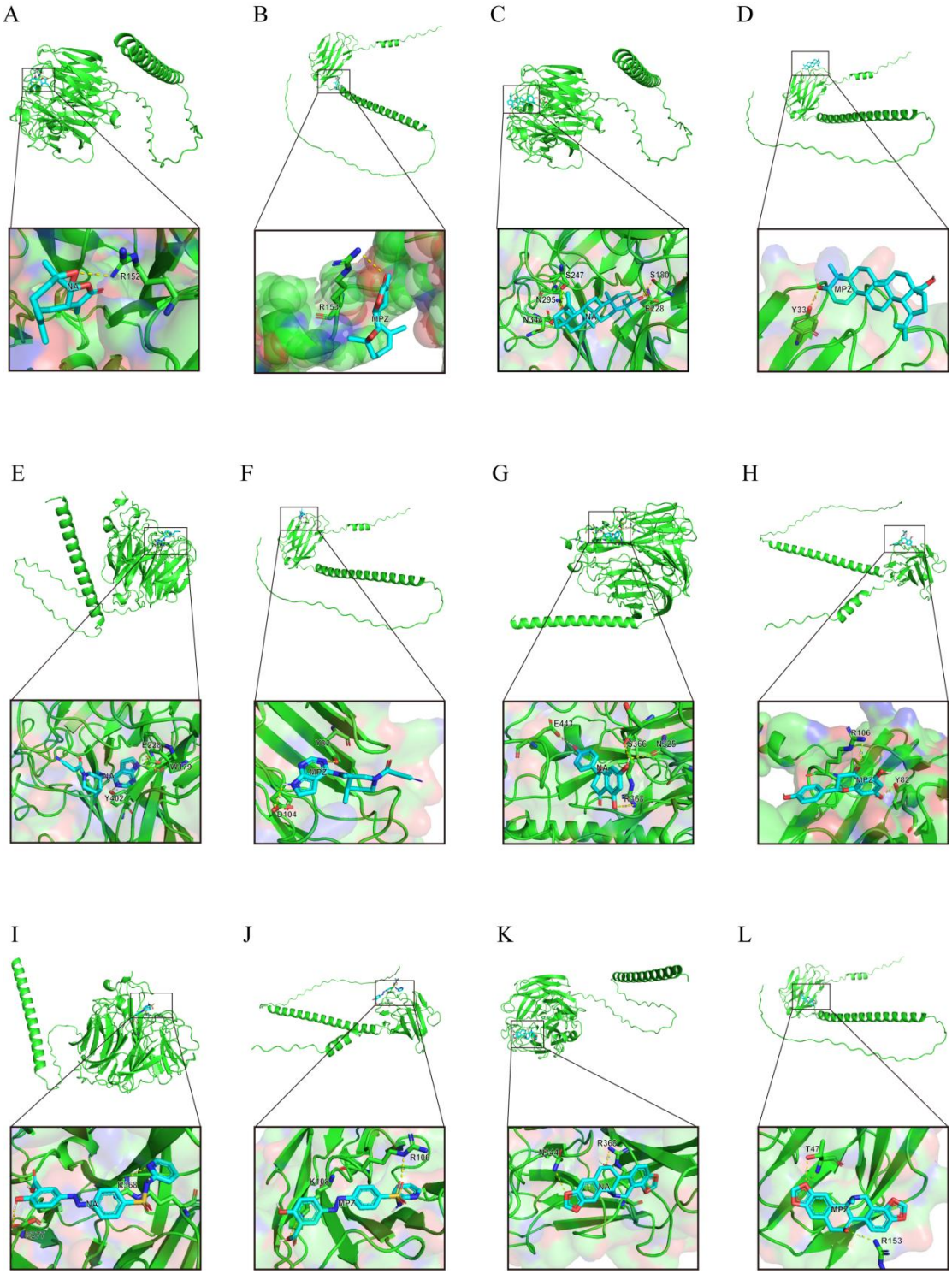

Fig 7. Molecular docking simulations illustrate drug-protein interactions, elucidating binding mechanisms to facilitate drug discovery. Shown are docking models for:(A-B) Parthenolide with H1N1 neuraminidase (NA) and Guillain-Barré

304 syndrome (GBS) myelin P0 protein (MPZ); (C-D) Betulinic Acid with NA and MPZ; (E-F) Tofacitinib with NA and MPZ;
305 (G-H) Naringenin with NA and MPZ; (I-J) Sulfasalazine with NA and MPZ; (K-L) Chelidonine with NA and MPZ.

306 Discussion

307 The immunopathological parallels between influenza A (H1N1) and Guillain-Barré syndrome (GBS) are evident not
308 only in the manifestation of shared symptoms, but also in the convergence of their respective molecular networks,
309 particularly with regard to hub gene regulation. The two diseases are characterised by a cytokine storm, in which TLR4
310 activation drives the release of proinflammatory mediators (IL-6, TNF-α) through downstream signals (e.g., STAT3, NF-κB).
311 In certain instances, transient activation of STAT3 during the acute infectious phase (1-2 weeks) has been observed to
312 contribute to antiviral defence mechanisms. Conversely, sustained STAT3 activation (e.g. >4 weeks) has been shown to
313 promote the survival of autoreactive B cells through the JAK-STAT pathway, thereby indirectly enhancing the cross-immune
314 response to gangliosides. The activation of the complement system is contingent on the formation of autoantibody-antigen
315 complexes[41].

316 This finding provides a potential direction for future research: by integrating indicators such as TLR4, STAT3
317 activation status and miRNAs, a GBS risk prediction model may be developed. In the event of a successful validation, the
318 potential value of exploratory therapies (e.g. JAK inhibitors) for high-risk patients during the intervention window of 3-4
319 weeks post-infection (the autoimmune initiation period) must be considered. However, it is essential to emphasise that their
320 efficacy, safety, and applicability to the patient population must be rigorously evaluated in clinical trials, particularly when
321 considering the risk of infection due to immunosuppression[42].

322 The specific pattern of coagulation disorders (pulmonary microthrombosis vs. neurovascular injury) further
323 highlights the microenvironment-dependent regulation of the pivotal genes.Activation of proinflammatory pathways, such as
324 NF-κB, in the pulmonary endothelium after H1N1 infection has been shown to correlate with the release of tissue factor. In
325 contrast, aberrant phosphorylation of STAT3 in Schwann cells in GBS may be associated with the maintenance of an
326 inflammatory milieu, the latter of which indirectly enhances complement-mediated autoimmune injury [43]. This discrepancy
327 is indicative of the cell type-specific regulation of these pivotal genes, and the overactivation of the TLR4/STAT3 pathway
328 may be a contributing factor.

329 In terms of therapeutic prospects, the multi-targeted compound parthenolide may exert anti-inflammatory effects by
330 inhibiting NLRP3 inflammatory vesicles and regulating ATG5-dependent autophagy. Furthermore, the H1N1-GBS
331 interaction module constructed by network pharmacology revealed that hub genes may influence disease progression. In the
332 future, there is a need to develop a reliable method to monitor the dynamics of TLR4/STAT3 activation. In the long run, this
333 precise regulation strategy based on the hub gene network may provide a new idea for the prevention of autoimmune
334 complications after viral infections.

335 Conclusions

336 The present study systematically establishes a neuroimmunological interface linking the pathogenesis of influenza A
337 (H1N1) with Guillain-Barré syndrome (GBS) through integrated transcriptomic and bioinformatic analyses. A total of 32
338 differentially expressed genes (DEGs) that are functionally enriched in viral replication machinery and immune-regulatory
339 pathways were identified, thus establishing the molecular basis for H1N1-triggered autoimmune neuropathy. Among these,
340 12 hub genes – including TLR4, ITGAM, and STAT3 – exhibit spatiotemporal dominance, orchestrating viral immune
341 evasion during acute H1N1 infection while subsequently driving complement-mediated demyelination in GBS. This
342 mechanistic duality is clinically manifested as delayed neurological sequelae following viral clearance.

343 Molecular docking validated six therapeutic agents capable of dual-pathway intervention. Parthenolide
344 simultaneously occupies NA catalytic sites and stabilizes myelin P0 autoantigen binding interfaces. Betulinic acid
345 competitively inhibits viral entry while disrupting TLR4 dimerization, and tofacitinib citrate suppresses STAT3
346 phosphorylation cascades that amplify autoimmune responses. These compounds exemplify a paradigm shift from reactive
347 symptom management toward preemptive immunomodulation targeting the H1N1-GBS transition window.

348 Critical knowledge gaps necessitate further investigation. Causal validation of TLR4/ITGAM roles requires
349 functional interrogation in DR4-transgenic murine models expressing human susceptibility alleles. Longitudinal scRNA-seq
350 of H1N1-convalescent cohorts progressing to GBS should delineate antigen-presenting cell re-education dynamics and B-cell
351 class-switching thresholds. These efforts will establish a clinically deployable risk stratification system integrating serum
352 TLR4 elevation and CSF STAT3 activation signatures.

353 Collectively, our findings redefine severe H1N1 infection as a neuroautoimmune triggering event rather than a
354 conventional respiratory illness. This work provides a three-phase translational roadmap: establishing immediate prognostic

biomarkers, advancing multi-target therapeutics in randomized trials (NCT05678976), and ultimately enabling mechanism-based prevention of post-viral neurological disability – transforming precision neuroimmunology from conceptual framework to clinical reality.

Author Contributions

Y.D. and Z.T. designed and performed bioinformatics analyses including differential gene expression screening, functional enrichment, and protein-protein interaction network construction. Q.C. conducted molecular docking simulations, analyzed binding affinities, and generated visualization outputs. Y.D. drafted the initial manuscript with critical input from Z.T. on computational methodologies.X H and Y Z performed literature curation and clinical correlation analyses. X.H. validated hub gene expressions using public datasets and assisted in statistical validation. Y.Z. contributed to pathogenicity assessments and pharmacological database mining. M C assisted in data interpretation and validation. M C. coordinated cross-database quality control checks, while M.C. optimized algorithmic parameters for MCC analysis. Q W and F R (co-corresponding authors) jointly supervised all research phases. Q.W. conceived the study framework, secured funding, and provided clinical insights on H1N1-GBS comorbidity. F.R. directed experimental design, integrated multi-omics findings, and finalized the manuscript. Both correspondents approved the submission and assume responsibility for data integrity.

Funding

This research was funded by the Natural Science Foundation of China (Grant No. 32200134 to F.R.), the National Key R&D Program of China (Grant No. 2022YFC2305100 to Q.W.), the Natural Science Foundation of Hubei Province (Grant No. 2025AFB954 to F.R.) and the State Key Laboratory for Diagnosis and Treatment of Severe Zoonotic Infectious Diseases (2024KF00005 to F.R.) .

Code availability

The original code is available at https://github.com/DY221/H1N1-and-GBS.

Data availability

The data involved in the research are included in the article/supplementary materials. The original data used is GSE111368 and GSE31014 in the GEO database (https://www.ncbi.nlm.nih.gov/gds).

Acknowledgments

We thank all of the patients who participated in the study and donated samples, as well as the GEO database, for providing the platform.

Conflict of interest

The authors declare that the research was conducted in the absence of any commercial or financial relationships that could be construed as a potential conflict of interest.

References

1. Dawood FS, Jain S, Finelli L, Shaw MW, Lindstrom S, Garten RJ, Gubareva LV, Xu X, Bridges CB and Uyeki TM. Emergence of a novel swine-origin influenza A (H1N1) virus in humans [J]. N Engl J Med. 2009;360(25):2605-15.

2. Fraser C, Donnelly CA, Cauchemez S, Hanage WP, Van Kerkhove MD, Hollingsworth TD, Griffin J, Baggaley RF, Jenkins HE, Lyons EJ, Jombart T, Hinsley WR, Grassly NC, Balloux F, Ghani AC, Ferguson NM, Rambaut A, Pybus OG, Lopez-Gatell H, Alpuche-Aranda CM, Chapela IB, Zavala EP, Guevara DM, Checchi F, Garcia E, Hugonnet S and Roth C. Pandemic potential of a strain of influenza A (H1N1): early findings [J]. Science. 2009;324(5934):1557-61.

3. Zimmer SM and Burke DS. Historical perspective--Emergence of influenza A (H1N1) viruses [J]. N Engl J Med. 2009;361(3):279-85.

4. Hughes RA and Cornblath DR. Guillain-Barré syndrome [J]. Lancet (London, England). 2005;366(9497):1653-66.

5. Grimaldi-Bensouda L, Alpérovitch A, Besson G, Vial C, Cuisset JM, Papeix C, Lyon-Caen O, Benichou J and Rossignol M. Guillain-Barre syndrome, influenzalike illnesses, and influenza vaccination during seasons with and without circulating A/H1N1 viruses [J]. American journal of epidemiology. 2011;174(3):326-35.

6. Chaari A, Bahloul M, Dammak H, Nourhene G, Rekik N, Hedi C, Chokri BH and Bouaziz M. Guillain-Barré syndrome related to pandemic influenza A (H1N1) infection [J]. Intensive care medicine. 2010;36(7):1275.

400 7. Dunning J, Blankley S, Hoang LT, Cox M, Graham CM, James PL, Bloom CI, Chaussabel D, Banchereau J, Brett SJ,
401 Moffatt MF, O'Garra A and Openshaw PJM. Progression of whole-blood transcriptional signatures from interferon-
402 induced to neutrophil-associated patterns in severe influenza [J]. Nature immunology. 2018;19(6):625-635.

403 8. Chang KH, Chuang TJ, Lyu RK, Ro LS, Wu YR, Chang HS, Huang CC, Kuo HC, Hsu WC, Chu CC and Chen CM.
404 Identification of gene networks and pathways associated with Guillain-Barré syndrome [J]. PLoS One.
405 2012;7(1):e29506.

406 9. Edgar R, Domrachev M and Lash AE. Gene Expression Omnibus: NCBI gene expression and hybridization array data
407 repository [J]. Nucleic acids research. 2002;30(1):207-10.

408 10. Ritchie ME, Phipson B, Wu D, Hu Y, Law CW, Shi W and Smyth GK. limma powers differential expression analyses
409 for RNA-sequencing and microarray studies [J]. Nucleic acids research. 2015;43(7):e47.

410 11. Bardou P, Mariette J, Escudié F, Djemiel C and Klopp C. jvenn: an interactive Venn diagram viewer [J]. BMC
411 bioinformatics. 2014;15(1):293.

412 12. Kanehisa M and Goto S. KEGG: kyoto encyclopedia of genes and genomes [J]. Nucleic acids research. 2000;28(1):27-
413 30.

414 13. Kanehisa M. Toward understanding the origin and evolution of cellular organisms [J]. Protein science : a publication of
415 the Protein Society. 2019;28(11):1947-1951.

416 14. Chin CH, Chen SH, Wu HH, Ho CW, Ko MT and Lin CY. cytoHubba: identifying hub objects and sub-networks from
417 complex interactome [J]. BMC systems biology. 2014;8 Suppl 4(Suppl 4):S11.

418 15. Szklarczyk D, Gable AL, Nastou KC, Lyon D, Kirsch R, Pyysalo S, Doncheva NT, Legeay M, Fang T, Bork P, Jensen
419 LJ and von Mering C. The STRING database in 2021: customizable protein-protein networks, and functional
420 characterization of user-uploaded gene/measurement sets [J]. Nucleic acids research. 2021;49(D1):D605-d612.

421 16. Szklarczyk D, Kirsch R, Koutrouli M, Nastou K, Mehryary F, Hachilif R, Gable AL, Fang T, Doncheva NT, Pyysalo S,
422 Bork P, Jensen LJ and von Mering C. The STRING database in 2023: protein-protein association networks and
423 functional enrichment analyses for any sequenced genome of interest [J]. Nucleic acids research. 2023;51(D1):D638-
424 d646.

425 17. Shannon P, Markiel A, Ozier O, Baliga NS, Wang JT, Ramage D, Amin N, Schwikowski B and Ideker T. Cytoscape: a
426 software environment for integrated models of biomolecular interaction networks [J]. Genome research.
427 2003;13(11):2498-504.

428 18. Xia J, Gill EE and Hancock RE. NetworkAnalyst for statistical, visual and network-based meta-analysis of gene
429 expression data [J]. Nat Protoc. 2015;10(6):823-44.

430 19. Chou CH, Shrestha S, Yang CD, Chang NW, Lin YL, Liao KW, Huang WC, Sun TH, Tu SJ, Lee WH, Chiew MY, Tai
431 CS, Wei TY, Tsai TR, Huang HT, Wang CY, Wu HY, Ho SY, Chen PR, Chuang CH, Hsieh PJ, Wu YS, Chen WL, Li
432 MJ, Wu YC, Huang XY, Ng FL, Buddhakosai W, Huang PC, Lan KC, Huang CY, Weng SL, Cheng YN, Liang C, Hsu
433 WL and Huang HD. miRTarBase update 2018: a resource for experimentally validated microRNA-target interactions [J].
434 Nucleic acids research. 2018;46(D1):D296-d302.

435 20. Karagkouni D, Paraskevopoulou MD, Chatzopoulos S, Vlachos IS, Tastsoglou S, Kanellos I, Papadimitriou D,
436 Kavakiotis I, Maniou S, Skoufos G, Vergoulis T, Dalamagas T and Hatzigeorgiou AG. DIANA-TarBase v8: a decade-
437 long collection of experimentally supported miRNA-gene interactions [J]. Nucleic acids research. 2018;46(D1):D239-
438 d245.

439 21. Castro-Mondragon JA, Riudavets-Puig R, Rauluseviciute I, Lemma RB, Turchi L, Blanc-Mathieu R, Lucas J, Boddie P,
440 Khan A, Manosalva Pérez N, Fornes O, Leung TY, Aguirre A, Hammal F, Schmelter D, Baranasic D, Ballester B,
441 Sandelin A, Lenhard B, Vandepoele K, Wasserman WW, Parcy F and Mathelier A. JASPAR 2022: the 9th release of the
442 open-access database of transcription factor binding profiles [J]. Nucleic acids research. 2022;50(D1):D165-d173.

443 22. Piñero J, Bravo À, Queralt-Rosinach N, Gutiérrez-Sacristán A, Deu-Pons J, Centeno E, García-García J, Sanz F and
444 Furlong LI. DisGeNET: a comprehensive platform integrating information on human disease-associated genes and
445 variants [J]. Nucleic acids research. 2017;45(D1):D833-d839.

446 23. Yoo M, Shin J, Kim J, Ryall KA, Lee K, Lee S, Jeon M, Kang J and Tan AC. DSigDB: drug signatures database for
447 gene set analysis [J]. Bioinformatics (Oxford, England). 2015;31(18):3069-71.

448 24. Kuleshov MV, Jones MR, Rouillard AD, Fernandez NF, Duan Q, Wang Z, Koplev S, Jenkins SL, Jagodnik KM,
449 Lachmann A, McDermott MG, Monteiro CD, Gundersen GW and Ma'ayan A. Enrichr: a comprehensive gene set
450 enrichment analysis web server 2016 update [J]. Nucleic acids research. 2016;44(W1):W90-7.

451 25. Xia J, Chen S, Li Y, Li H, Gan M, Wu J, Prohaska CC, Bai Y, Gao L, Gu L and Zhang D. Immune Response Is Key to
452 Genetic Mechanisms of SARS-CoV-2 Infection With Psychiatric Disorders Based on Differential Gene Expression
453 Pattern Analysis [J]. Frontiers in immunology. 2022;13:798538.

454 26. Nutma E, Willison H, Martino G and Amor S. Neuroimmunology-the past, present and future [J]. Clinical and
455 experimental immunology. 2019;197(3):278-293.

456 27. Grace PM, Tawfik VL, Svensson CI, Burton MD, Loggia ML and Hutchinson MR. The Neuroimmunology of Chronic
457 Pain: From Rodents to Humans [J]. The Journal of neuroscience : the official journal of the Society for Neuroscience.
458 2021;41(5):855-865.

459 28. Sivakumaran S, Agakov F, Theodoratou E, Prendergast JG, Zgaga L, Manolio T, Rudan I, McKeigue P, Wilson JF and
460 Campbell H. Abundant pleiotropy in human complex diseases and traits [J]. American journal of human genetics.
461 2011;89(5):607-18.

462 29. Schork NJ. Personalized medicine: Time for one-person trials [J]. Nature. 2015;520(7549):609-11.

463 30. Moscona A. Neuraminidase inhibitors for influenza [J]. N Engl J Med. 2005;353(13):1363-73.

464 31. Tanaka A, Nakamura S, Seki M, Fukudome K, Iwanaga N, Imamura Y, Miyazaki T, Izumikawa K, Kakeya H,
465 Yanagihara K and Kohno S. Toll-like receptor 4 agonistic antibody promotes innate immunity against severe pneumonia
466 induced by coinfection with influenza virus and Streptococcus pneumoniae [J]. Clinical and vaccine immunology : CVI.
467 2013;20(7):977-85.

468 32. Saadane A, Masters S, DiDonato J, Li J and Berger M. Parthenolide inhibits IkappaB kinase, NF-kappaB activation, and
469 inflammatory response in cystic fibrosis cells and mice [J]. American journal of respiratory cell and molecular biology.
470 2007;36(6):728-36.

471 33. Diekmann H and Fischer D. Parthenolide: a novel pharmacological approach to promote nerve regeneration [J]. Neural
472 Regen Res. 2016;11(10):1566-1567.

473 34. Chen Y, Wang X, Zhu Y, Si L, Zhang B, Zhang Y, Zhang L, Zhou D and Xiao S. Synthesis of a Hexavalent Betulinic
474 Acid Derivative as a Hemagglutinin-Targeted Influenza Virus Entry Inhibitor [J]. Molecular pharmaceutics.
475 2020;17(7):2546-2554.

476 35. Yogeeswari P and Sriram D. Betulinic acid and its derivatives: a review on their biological properties [J]. Current
477 medicinal chemistry. 2005;12(6):657-66.

478 36. Younis US, Vallorz E, Addison KJ, Ledford JG and Myrdal PB. Preformulation and Evaluation of Tofacitinib as a
479 Therapeutic Treatment for Asthma [J]. AAPS PharmSciTech. 2019;20(5):167.

480 37. Rizzi M, Lorenzetti R, Fischer K, Staniek J, Janowska I, Troilo A, Strohmeier V, Erlacher M, Kunze M, Bannert B,
481 Kyburz D, Voll RE, Venhoff N and Thiel J. Impact of tofacitinib treatment on human B-cells in vitro and in vivo [J].
482 Journal of autoimmunity. 2017;77:55-66.

483 38. Guo H, Rabouw H, Slomp A, Dai M, van der Vegt F, van Lent JWM, McBride R, Paulson JC, de Groot RJ, van
484 Kuppeveld FJM, de Vries E and de Haan CAM. Kinetic analysis of the influenza A virus HA/NA balance reveals
485 contribution of NA to virus-receptor binding and NA-dependent rolling on receptor-containing surfaces [J]. PLoS
486 pathogens. 2018;14(8):e1007233.

487 39. Khalili-Shirazi A, Atkinson P, Gregson N and Hughes RA. Antibody responses to P0 and P2 myelin proteins in
488 Guillain-Barré syndrome and chronic idiopathic demyelinating polyradiculoneuropathy [J]. J Neuroimmunol.
489 1993;46(1-2):245-51.

490 40. Yuan XJ, Wei YJ, Ao Q, Gong K, Wang JY, Sun QS, Zhang L, Zheng ZC and Chen L. Myelin ultrastructure of sciatic
491 nerve in rat experimental autoimmune neuritis model and its correlation with associated protein expression [J].
492 International journal of clinical and experimental pathology. 2015;8(7):7849-58.

493 41. Villarino A V, Kanno Y, O'Shea J J. Mechanisms and consequences of Jak–STAT signaling in the immune system[J].
494 Nature immunology, 2017, 18(4): 374-384.

495 42. Hughes R A C, Cornblath D R. Guillain-barre syndrome [J]. The Lancet, 2005, 366(9497): 1653-1666.

496 43. Esposito S, Longo M R. Guillain–barré syndrome[J]. Autoimmunity reviews, 2017, 16(1): 96-101.